Decreased Basal Ganglia Volume in Cerebral Amyloid Angiopathy

Panagiotis Fotiadis,[a,b] Marco Pasi,[a,c] Andreas Charidimou,[a] Andrew D. Warren,[a] Kristin M. Schwab,[a] Alzheimer's Disease Neuroimaging Initiative,* Jonathan Rosand,[a] Jeroen van der Grond,[d] Mark A. van Buchem,[d] Anand Viswanathan,[a] M. Edip Gurol,[a] Steven M. Greenberg[a]

[a]Department of Neurology, J.P. Kistler Stroke Research Center, Massachusetts General Hospital, Harvard Medical School, Boston, MA, USA
[b]Department of Neuroscience, Perelman School of Medicine, University of Pennsylvania, Philadelphia, PA, USA
[c]Stroke Unit, Department of Neurology, University of Lille, INSERM U1171, CHU Lille, Lille, France
[d]Department of Radiology, Leiden University Medical Center, Leiden, the Netherlands

Background and Purpose Cerebral amyloid angiopathy (CAA) is a common pathology of the leptomeningeal and cortical small vessels associated with hemorrhagic and non-hemorrhagic brain injury. Given previous evidence for CAA-related loss of cortical thickness and white matter volume, we hypothesized that CAA might also cause tissue loss in the basal ganglia.

Methods We compared basal ganglia volumes expressed as a percentage of total intracranial volume (pBGV) of non-demented patients with sporadic and hereditary CAA to age-matched healthy control (HC) and Alzheimer's disease (AD) cohorts.

Results Patients with sporadic CAA had lower pBGV (n=80, 1.16%±0.14%) compared to HC (n=80, 1.30%±0.13%, $P<0.0001$) and AD patients (n=80, 1.23%±0.11%, $P=0.001$). Similarly, patients with hereditary CAA demonstrated lower pBGV (n=25, 1.26%±0.17%) compared to their matched HC (n=25, 1.36%±0.15%, $P=0.036$). Using a measurement of normalized basal ganglia width developed for analysis of clinical-grade magnetic resonance images, we found smaller basal ganglia width in patients with CAA-related lobar intracerebral hemorrhage (ICH; n=93, 12.35±1.47) compared to age-matched patients with hypertension-related deep ICH (n=93, 13.46±1.51, $P<0.0001$) or HC (n=93, 15.45±1.22, $P<0.0001$). Within the sporadic CAA research cohort, decreased basal ganglia volume was independently correlated with greater cortical gray matter atrophy (r=0.45, $P<0.0001$), increased basal ganglia fractional anisotropy (r=−0.36, $P=0.001$), and worse performance on language processing (r=0.35, $P=0.003$), but not with cognitive tests of executive function or processing speed.

Conclusions These findings suggest an independent effect of CAA on basal ganglia tissue loss, indicating a novel mechanism for CAA-related brain injury and neurologic dysfunction.

Keywords Cerebral amyloid angiopathy; Basal ganglia; Atrophy; Diffusion; Cognition

JoS

Fotiadis et al.   Basal Ganglia Atrophy in Cerebral Amyloid Angiopathy

Introduction

Although brain atrophy, defined as loss of brain volume unrelated to a defined macroscopic injury,[1] is a prominent feature of neurodegenerative disease, it can also reflect cerebrovascular disease. Reduced overall brain volume[2] as well as specific reductions in white matter volume (WMV)[3] or cortical thickness[4] have been observed in various small vessel diseases, often correlating with measures of cognitive impairment. Atrophy of the basal ganglia, however, has generally not been analyzed in the setting of cerebral small vessel disease.

Cerebrovascular β-amyloid deposition or cerebral amyloid angiopathy (CAA) is a common pathology of the leptomeningeal and cortical small vessels that has been linked to cortical hemorrhagic lesions as well as non-hemorrhagic cortical injury such as brain atrophy. Analysis of patients diagnosed with sporadic CAA by validated clinical criteria or with hereditary CAA by genetic testing has found thinning of the cerebral cortex in both groups.[5] Despite its localization to leptomeningeal and cortical small vessels, CAA also appears to cause substantial non-hemorrhagic damage to subcortical structures, including increased white matter hyperintensities of presumed vascular origin,[6] lower supratentorial WMVs,[7] changes in white matter diffusion-tensor imaging (DTI) properties,[8,9] and white matter microinfarcts.[10,11] The likeliest mechanism for CAA-related non-hemorrhagic brain injury appears to be vascular dysfunction[12,13] leading to tissue ischemia. Although few studies have searched for effects of CAA on subcortical gray matter structures such as the basal ganglia, an early DTI study of this disorder reported increased fractional anisotropy (FA) of subthalamic gray matter.[8]

Based on the association of CAA with volume loss in cortex and white matter, we sought to determine its relationship to basal ganglia volume (BGV). The basal ganglia, typically defined as putamen, caudate, globus pallidus, and nucleus accumbens, are a set of interconnected deep gray matter nuclei thought to regulate a range of complex functions including voluntary and involuntary motor control,[14] non-declarative memory and habit formation,[15] language processing,[16] action selection,[17] and emotional perception.[18] Basal ganglia damage is a prominent early manifestation of neurodegenerative disorders such as Parkinson's disease,[19] progressive supranuclear palsy,[20] and Huntington's disease,[21] where it is felt to mediate neurocognitive as well as movement-related clinical symptoms.[22] From a clinical standpoint, the current finding of CAA-related loss of BGV could represent a novel mechanism for mediating a portion of the cognitive and motor impairments related to this common small vessel pathology and thus an imaging marker for assessing CAA's impact and its response to candidate interventions.

Methods

Study design and participants

Research cohorts

Individuals (n=80) with sporadic CAA were prospectively enrolled at Massachusetts General Hospital, in Boston, MA, between March 15, 2006 and December 1, 2014. Each individual was non-demented and carried a diagnosis of probable CAA per the pathologically validated modified Boston criteria.[23] Demographic and clinical data were collected for each patient at the time of enrollment.

Of the 80 research patients with sporadic CAA, 68 agreed to undergo a standard neurocognitive battery. Executive function (Trail Making test B, Digit Span test backwards, verbal fluency test), processing speed (Trail Making Test A, Symbol Substitution test), verbal memory (immediate and delayed memory scores based on Hopkins Verbal Learning test), and language processing (Animal Naming test, Boston naming test) z-scores were calculated using the mean and standard deviation scores from the entire sporadic CAA cohort, as described.[9] Gait velocity and time were determined using the Timed Get Up and Go test (n=62).[9]

Individuals in the research CAA cohort were age-matched to healthy controls (HC; n=80) and patients with Alzheimer's disease (AD; n=80) collected from the Alzheimer's Disease Neuroimaging Initiative (ADNI).[24] Of the 80 AD patients collected from ADNI, 46 (57.5%) had a clinical dementia rating score of 0.5; the remaining 34 had a clinical dementia rating score of 1.

Individuals with the Dutch-type hereditary form of CAA (D-CAA, previously known as Hereditary Cerebral Hemorrhage With Amyloidosis—Dutch or HCHWA-D) were prospectively enrolled at the Leiden University Medical Center and the diagnosis confirmed by genetic testing.[5,25] The D-CAA patients (n=25) were age-matched to genetically verified mutation-negative HCs (n=25) enrolled at the same center. Of the 25 enrolled D-CAA patients, 14 presented clinically with lobar intracerebral hemorrhage (ICH) and 10 were presymptomatic carriers of the D-CAA-associated gene mutation. Demographic and clinical data were similarly collected for the D-CAA patients.[25]

Cohorts with clinical grade magnetic resonance images

In addition to the above cohorts that received high-resolution

dedicated research magnetic resonance images (MRIs), we analyzed clinical MRIs of patients who were admitted to Massachusetts General Hospital between January, 2003 and February, 2012, with spontaneous symptomatic ICH. Patients in this group were categorized as having definite or probable CAA-related lobar ICH (CAA-ICH: n=93), and age-matched patients with hypertensive arteriopathy and ICH (HTN-ICH: n=93). The latter group consisted of patients with ICH in the basal ganglia, thalamus, or brainstem but not lobar ICH, as described.[26] All analyses were performed on non-ICH containing hemispheres; patients with bilateral ICHs were excluded. Demographic and clinical information was obtained for those patients at the time of enrollment.[26]

Age-matching was performed based on the closest first decimal of age without knowledge of clinical or radiological information.[5] The Institutional Review Boards of the participating sites approved this study and all patients provided signed written informed consent.

MRI acquisition

The research cohort of sporadic CAA patients underwent structural MRI using a Siemens Avanto 1.5T scanner (12-channel head coil; Siemens Healthineers, Erlangen, Germany). The standardized battery included T1-weighted Multi-echo Magnetization–Prepared Rapid Gradient Echo (voxel size 1×1×1 mm³; repetition time [TR], 2,730 ms; inversion time [TI], 1,100 ms), high-resolution susceptibility weighted imaging (SWI; voxel size 0.75×0.75×1.3 mm³; TR, 48 ms; echo time [TE], 40 ms), three-dimensional fluid attenuated inversion recovery (FLAIR; voxel size 1×1×1 mm³; TR, 6,000 ms; TE, 302 ms; TI, 2,200 ms), and high-resolution Diffusion (voxel size 2×2×2 mm³; TR, 8,180 ms; TE, 82 ms; 60 directions; b-value=700; 10 b_0 images) sequences.

HCs and patients with AD selected from the ADNI database underwent a similar structural MRI protocol using Siemens 1.5T scanners.[5,24]

Patients diagnosed with D-CAA and their matched controls underwent research structural MRI using a Philips 3T scanner (Philips Healthcare, Andover, MA, USA). The MRI protocol included 3D T1-weighted (voxel size 0.875×0.875×1.2 mm³; TR, 9 ms; TE, 4.6 ms), SWI (voxel size 0.7812×0.7812×0.8 mm³; TR, 45 ms; TE, 31 ms), and FLAIR (voxel size 0.4297×0.4297×5.5 mm³; TR, 11 ms; TE, 125 ms) sequences.

The clinical cohorts of patients with CAA-ICH or HTN-ICH underwent a structural MRI protocol using a General Electric Sigma 1.5T scanner (GE Healthcare, Barrington, IL, USA). The clinical MRI protocols included T1-weighted, T2*-weighted Gradient-Recalled Echo, and FLAIR sequences, as described.[26]

MRI processing

Structural analyses

Segmentation of cortical gray, white, and basal ganglia structures as well as estimated total intracranial volume (eTIV) were performed using FreeSurfer version 5.3.0 (https://surfer.nmr.mgh.harvard.edu). Cortical gray matter volume (CGMV) was defined as the volume between the pial surface and gray-white junction, measured using a surface-based approach[27] and expressed as a percent of intracranial volume (pCGMV). Similarly, WMV was defined as the volume enclosed within the gray-white junction minus any non-white matter entities such as the subcortical gray matter structures and the ventricles and expressed as a percent of intracranial volume (pWMV). The basal ganglia volume was defined as the sum of the putamen, caudate nucleus, globus pallidus, and nucleus accumbens volumes, and expressed as a percent of intracranial volume (pBGV). White matter hyperintensity volume, a marker of CAA-related structural injury, was estimated using a previously validated semi-automated algorithm, and expressed as a percentage of eTIV (pWMH).[6]

Diffusion analyses

High-resolution diffusion scans were preprocessed using the 'dt_recon' pipeline of FreeSurfer. Preprocessing of the scans consisted of correcting eddy currents and head motion artifacts while registering all diffusion scans to a common anatomical template. After manually confirming accurate co-registration between the diffusion and anatomical scans, the resulting FA and apparent diffusion coefficient (ADC) volumetric heat maps were used to calculate the FA and ADC values within the putamen, caudate nucleus, globus pallidus, and nucleus accumbens. Basal ganglia FA and ADC values were defined as the volume-weighted average FA and ADC of those sub-structures.

All segmentation outputs and results were manually checked to ensure accuracy and manual interventions were performed when necessary.[5] Whenever gross pathology (i.e., ICH) was present in either hemisphere (n=40), results were obtained only from the contralateral hemisphere.

Normalized basal ganglia width

To assess basal ganglia atrophy in ICH patients with clinical-grade MRI scans not suitable for FreeSurfer-based volumetric measurement, we developed a metric based on the sum of the widths of three basal ganglia substructures—the caudate nucleus, putamen, and globus pallidus—normalized to the intracranial diameter (Figure 1). The measurement was obtained

JoS

Fotiadis et al.   Basal Ganglia Atrophy in Cerebral Amyloid Angiopathy

from the axial slice containing the largest area of the putamen, anterior commissure, septum pellucidum, and the pulvinar of thalamus[28] in the ICH-free hemisphere of each subject's axial T1-weighted sequence. An experienced rater (P.F.) determined normalized basal ganglia width on the 93 CAA-ICH and 93 HTN-ICH clinical cases of interest. For comparison to HCs, we applied the same basal ganglia width metric to MRI scans from 93 HC obtained from ADNI (Table 1). To test the metric's reliability, a second rater (M.P.) independently measured 30 randomly selected CAA-ICH cases and 30 randomly selected HTN-ICH cases. For these 60 scans, the intraclass correlation coefficient (two-way random effects model, consistency, single measures; SPSS software suite version 25, IBM Co., Armonk, NY, USA) was 0.847 (95% confidence interval [CI], 0.756 to

0.906). To assess the validity of the developed basal ganglia visual atrophy scale to accurately estimate BGV, we applied it on the research-quality ADNI HC cohort (n=93) and compared it to their corresponding FreeSurfer-derived pBGV. The Pearson's correlation between the visual atrophy scale and the automated volumetric measurements was r=0.22 (P=0.037).

Statistical analyses

Statistical analyses were performed using the JMP Statistical Software by SAS version Pro 14.0 (SAS Institute Inc., Cary, NC, USA). Bivariate correlation analyses were carried out in the form of two-tailed t-tests (threshold for significance, $P<0.05$), and Pearson's correlation coefficients (r). The 240 research subjects (80 sporadic CAA patients, 80 matched HC, and 80 matched AD patients) were included in a general linear model with pBGV as the dependent variable, the binary diagnostic status ("CAA" vs. "HC" vs. "AD") as the class variable, and other potential confounders (age, sex, presence of hypertension, hyperlipidemia, and diabetes mellitus) as covariates. Tukey's test was used to correct for multiple comparisons between the three groups. Multiple linear regression models were additionally implemented to examine the independent relationship between the dependent variable pBGV and other variables of interest, after adjusting for the potentially confounding effects of age, sex, presence of hypertension, hyperlipidemia, and diabetes mellitus. Standardized regression coefficients (β), 95% CI, and P-values are reported for each multiple regression model. All volumetric variables examined were normally distributed.

A separate Bayesian appearance model was implemented
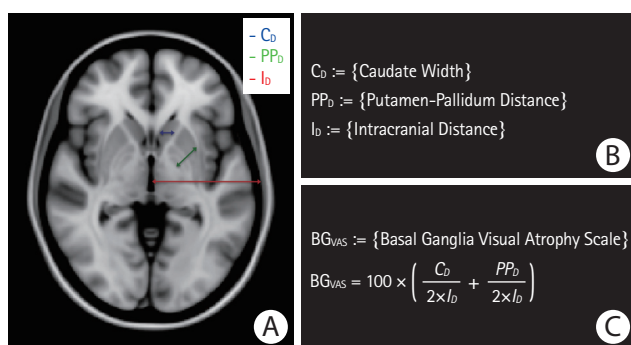
Figure 1. Visual basal ganglia atrophy scale. (A) Paradigm illustrating the three widths of interest: estimated caudate width (indicated in blue), estimated putamen-pallidum distance (indicated in green), and estimated hemispheric intracranial distance (indicated in red). (B) Definitions of the three widths of interest. (C) Definition of the normalized basal ganglia visual atrophy scale.

$C_D := \{\text{Caudate Width}\}$
$PP_D := \{\text{Putamen-Pallidum Distance}\}$
$I_D := \{\text{Intracranial Distance}\}$

$BG_{VAS} := \{\text{Basal Ganglia Visual Atrophy Scale}\}$
$BG_{VAS} = 100 \times \left(\dfrac{C_D}{2 \times I_D} + \dfrac{PP_D}{2 \times I_D} \right)$

Table 1. Comparison in normalized basal ganglia width in clinical cohorts

Variable	CAA-ICH	HTN-ICH	Healthy controls
No. of individuals	93	93	93
Demographics			
Age (yr)	68.5±7.1*	68.5±12.3*	73.1±3.3
Female sex	44 (47.3)	43 (46.2)	43 (46.2)
Hypertension	61 (65.6)[†,‡]	75 (80.7)[†]	0 (0)
Hyperlipidemia	40 (43)	38 (40.9)	42 (45.2)
Diabetes mellitus	11 (11.8)[†]	24 (25.8)[†]	9 (9.7)
Previous hemorrhagic stroke	17 (19.5)[†,§]	8 (9.1)[†]	0 (0)
Previous ischemic stroke	6 (6.5)[†]	10 (10.8)[†]	0 (0)
Basal ganglia visual atrophy scale			
Normalized basal ganglia width	12.35±1.47*,[‡]	13.46±1.51*	15.45±1.22

Values are presented as mean±standard deviation or number (%).
CAA-ICH, cerebral amyloid angiopathy-related intracerebral hemorrhage; HTN-ICH, hypertensive arteriopathy-related intracerebral hemorrhage.
*Denotes significantly less than healthy controls ($P\leq0.002$); [†]Denotes significantly higher than Healthy Controls ($P<0.05$); [‡]Denotes significantly less than patients with HTN-ICH ($P\leq0.002$); [§]Denotes significantly higher than patients with HTN-ICH ($P<0.05$).

using Functional Magnetic Resonance Imaging of the Brain (FMRIB) Software Library (FSL) FMRIB's Integrated Registration and Segmentation Tool (FIRST) automated toolbox in order to schematically explore the regional differences in volume between the basal ganglia and their individual components in patients with CAA, HC, and patients with AD. Topographical maps were generated using a threshold of $P<0.05$, corrected for multiple comparisons.

Results

Decreased basal ganglia volume in CAA
The research cohort consisted of 80 non-demented patients with sporadic CAA (mean age, 70.3±8.5 years), 80 age-matched HC (71.8±3.7), and 80 age-matched patients with AD (70.4±6.8). Detailed demographic and clinical information for these cohorts are provided in Table 2.

Sporadic CAA patients had lower pBGV than both HC (10.7% lower, $P<0.0001$) and patients with AD (5.4% lower, $P=0.001$). Atrophy was identified in the putamen, caudate nucleus, and globus pallidus (Table 3, Figures 2 and 3). Reduced pBGV in CAA relative to HC (pairwise difference=−0.13; 95% CI, −0.18 to −0.09; $P<0.0001$) and AD (pairwise difference=−0.05; 95% CI, −0.10 to −0.01; $P=0.016$) remained independent after controlling for age, sex, presence of hypertension, hyperlipidemia, and diabetes mellitus, using a general linear model adjusting for multiple comparisons (Tukey's). Other variables in this model correlating with decreased pBGV were male sex (pairwise difference=−0.10; 95% CI, −0.13 to −0.07; $P<0.0001$) and presence of hypertension (pairwise difference=−0.05; 95% CI, −0.08 to −0.01; $P=0.005$).

In a secondary analysis of basal ganglia atrophy relative to total brain atrophy, BGV was expressed as a percentage of total brain volume (defined as the sum of cortical gray matter and WMVs) and compared between the three cohorts. In bivariate analyses, patients with CAA had lower BGV expressed as a per-

centage of total brain volume compared to both HC (4.1% lower, $P=0.015$) and patients with AD (3.8% lower, $P=0.024$). The association between BGV expressed as a percentage of total brain volume and diagnostic group did not remain significant at the $P<0.05$ threshold (CAA vs. HC pairwise difference=−0.08; 95% CI, −0.17 to 0.01; $P=0.08$) (CAA vs. AD pairwise difference=−0.07; 95% CI, −0.15 to 0.02; $P=0.17$) after correcting for age, sex, presence of hypertension, hyperlipidemia, and diabetes mellitus (general linear model adjusting for multiple comparisons – Tukey's).

To further exclude confounding due to the presence of ICH or hypertension, we repeated these analyses in the subgroup of 40 CAA patients (mean age, 71.3±8.1) without ICH versus their corresponding age-matched HC and AD patients, and the subgroup of 34 non-hypertensive patients with sporadic CAA (67.9±8.3) versus their corresponding non-hypertensive age-matched HC and AD patients. In both subgroup analyses, patients with sporadic CAA had lower pBGV versus their comparator subgroups (Table 3).

We performed similar analyses of BGV in patients with D-CAA (n=25; mean age, 46.0±14.2) and their corresponding age-matched HC (n=25; mean age, 46.0±11.5). D-CAA patients demonstrated lower pBGV than their matched HC (decrease by 7.2%, $P=0.036$) (Table 3). This association was again independent of age, sex, presence of hypertension, hyperlipidemia, and diabetes mellitus (pairwise difference=−0.09; 95% CI, −0.17 to −0.01; $P=0.029$). In the same model, increased age was also independently correlated with smaller pBGV (β=−0.43; 95% CI, −0.62 to −0.14; $P=0.003$). Decreased pBGV in the D-CAA individuals was localized to the putamen ($P=0.030$) and the nucleus accumbens ($P=0.049$) with trend towards smaller globus pallidus ($P=0.083$) but not caudate nucleus ($P=0.42$).

To analyze for basal ganglia atrophy using clinical (rather than research-quality) MRI scans from patients with CAA-ICH and HTN-ICH, we developed a reproducible technique (see Methods) for measuring the normalized width of the caudate,

Table 2. Demographics and clinical information in research cohorts

Variable	Sporadic cohorts			Dutch cohorts	
	Sporadic CAA	Healthy controls	AD	D-CAA	Healthy controls
No. of individuals	80	80	80	25	25
Age (yr)	70.3±8.5	71.8±3.7	70.4±6.8	46±14.2	46±11.5
Female sex	18 (22.5)	36 (45.0)	35 (43.8)	15 (60.0)	17 (68.0)
Hypertension	46 (57.5)	30 (37.5)	39 (48.8)	6 (24.0)	4 (16.0)
Hyperlipidemia	36 (45.0)	42 (52.5)	45 (57.0)	5 (20.0)	2 (8.0)
Diabetes mellitus	6 (7.5)	9 (11.3)	6 (7.6)	2 (8.0)	0 (0)

Values are presented as mean±standard deviation or number (%).
CAA, cerebral amyloid angiopathy; AD, Alzheimer's disease; D-CAA, Dutch-type hereditary cerebral amyloid angiopathy.

JoS

Fotiadis et al.   Basal Ganglia Atrophy in Cerebral Amyloid Angiopathy

Table 3. Basal ganglia volumes in research cohorts

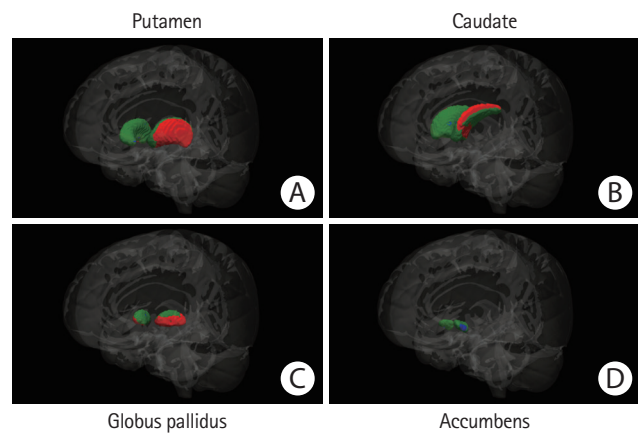| Variable	Sporadic cohorts			Dutch cohorts	
	Sporadic CAA	Healthy controls	AD	D-CAA	Healthy controls
All individuals					
Basal ganglia volume (% of eTIV)	1.16±0.14*,†	1.30±0.13	1.23±0.11*	1.26±0.17*	1.36±0.15
Putamen volume (% of eTIV)	0.54±0.08*,†	0.60±0.07	0.57±0.07*	0.58±0.12*	0.64±0.09
Caudate volume (% of eTIV)	0.40±0.07*,†	0.46±0.06	0.43±0.05*	0.46±0.05	0.48±0.06
Pallidus volume (% of eTIV)	0.17±0.02*,†	0.19±0.02	0.18±0.02	0.16±0.03	0.17±0.02
Accumbens volume (% of eTIV)	0.053±0.015	0.056±0.012	0.047±0.011*,†	0.055±0.015*	0.063±0.013
Sporadic CAA without intracerebral hemorrhage (n=40 for each group)					
Basal ganglia volume (% of eTIV)	1.16±0.15*,†	1.30±0.14	1.22±0.09*	-	-
Sporadic CAA without hypertension (n=34 for each group)					
Basal ganglia volume (% of eTIV)	1.16±0.16*,†	1.28±0.13	1.24±0.12	-	-

Values are presented as mean±standard deviation.
CAA, cerebral amyloid angiopathy; AD, Alzheimer's disease; D-CAA, Dutch-type hereditary cerebral amyloid angiopathy; eTIV, estimated total intracranial volume.
*Denotes significantly less than healthy controls ($P<0.05$); †Denotes significantly less than patients with AD ($P<0.05$); †Denotes significantly less than patients with CAA ($P<0.05$).
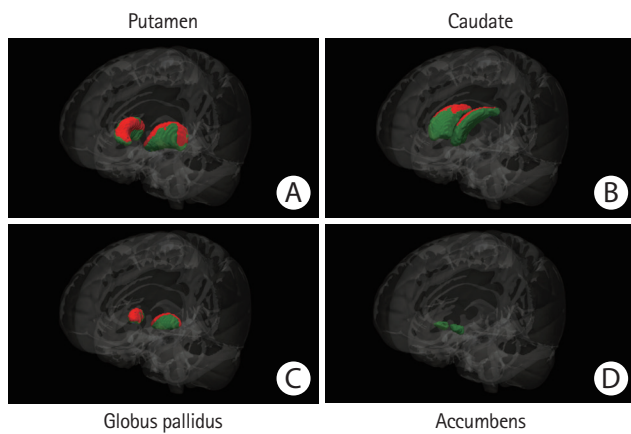
Figure 2. Regional basal ganglia atrophy in patients with sporadic cerebral amyloid angiopathy (CAA) versus healthy controls. The colored (green and red) regions represent masks of the (A) putamen, (B) caudate nucleus, (C) globus pallidus, or (D) nucleus accumbens. Red regions represent the locations where patients with sporadic CAA demonstrated significant atrophy when compared to age-matched healthy controls ($P<0.05$, corrected for multiple comparisons). Green regions represent the locations with no significant difference between the compared groups. The Functional Magnetic Resonance Imaging of the Brain (FMRIB) Software Library (FSL) FMRIB's Integrated Registration and Segmentation Tool (FIRST) for automatic segmentation of subcortical structures was used to generate the results. All results were manually checked to ensure accuracy, and the statistical maps were corrected for total intracranial volume.

Figure 3. Regional basal ganglia atrophy in patients with sporadic cerebral amyloid angiopathy (CAA) versus patients with Alzheimer's disease (AD). The colored (green, red, and blue) regions represent masks of the (A) putamen, (B) caudate nucleus, (C) globus pallidus, or (D) nucleus accumbens. Red regions represent the locations where patients with sporadic CAA demonstrated significant atrophy when compared to age-matched patients with AD, blue regions the locations where patients with AD demonstrated significant atrophy when compared to their matched CAA patients ($P<0.05$, corrected for multiple comparisons). Green regions represent the locations with no significant difference between the compared groups. The Functional Magnetic Resonance Imaging of the Brain (FMRIB) Software Library (FSL) FMRIB's Integrated Registration and Segmentation Tool (FIRST) for automatic segmentation of subcortical structures was used to generate the results. All results were manually checked to ensure accuracy, and the statistical maps were corrected for total intracranial volume.

putamen, and globus pallidus. Patients with CAA-ICH (n=93; mean age, 68.5±7.1) were compared to similar aged patients with HTN-ICH (n=93; 68.5±12.3) and an ADNI HC cohort (n=93; 73.1±3.3) (Table 1). Patients with CAA-ICH had greater

basal ganglia atrophy versus HTN-ICH (8.3% decrease in normalized basal ganglia width, $P<0.0001$) and both ICH groups had greater basal ganglia atrophy versus HC (CAA-ICH vs. HC: 20.1% decrease, HTN-ICH vs. HC: 12.9% decrease, $P<0.0001$

for both comparisons) (Table 1). Using a general linear model adjusting for multiple comparisons, the association between CAA-ICH and greater basal ganglia atrophy was again independent after correcting for age, sex, presence of hypertension, hyperlipidemia, and diabetes mellitus, as well as history of prior ICH and ischemic stroke (CAA-ICH vs. HTN-ICH pairwise difference=–1.11; 95% CI, –1.61 to –0.62 and CAA-ICH vs. HC pairwise difference=–3.18; 95% CI, –3.82 to –2.53; $P<0.0001$ for both comparisons). In the same model, male sex was independently associated with decreased BGV (pairwise difference=0.84; 95% CI, 0.52 to 1.17; $P<0.0001$).

Basal ganglia volume and other markers of structural integrity

We previously reported CAA-related cortical and white matter atrophy[5,7] as well as elevations in subcortical gray matter FA[8] and explored the association of these parameters with CAA-related basal ganglia atrophy. Among sporadic CAA patients, reduced pBGV correlated with pCGMV (r=0.45, $P<0.0001$) but not pWMV (r=0.18, $P=0.12$) or pWMH (r=0.02, $P=0.85$). The positive correlation between pBGV and pCGMV remained independent after adjusting for age, sex, presence of hypertension, hyperlipidemia, and diabetes mellitus (β=0.33; 95% CI, 0.05 to 0.65; $P=0.011$). The same subjects demonstrated a negative correlation between pBGV and basal ganglia FA (r=–0.36, $P=0.001$), and no association between pBGV and basal ganglia ADC (r=0.05, $P=0.68$). The correlation between pBGV and basal ganglia FA was also independent of age, sex, presence of hypertension, hyperlipidemia, and diabetes mellitus (β=–0.24; 95% CI, –0.45 to 0.03; $P=0.031$).

Basal ganglia volume and neurologic function

Because of the association of CAA with cognitive impairment,[29] we performed an exploratory analysis of the relationship between BGV and cognitive performance. Among the research cohort sporadic CAA patients who underwent complete neurocognitive assessment (n=68), there was a positive correlation between pBGV and verbal memory (r=0.26, $P=0.034$) and language processing (r=0.35, $P=0.003$), but not with executive function (r=–0.05, $P=0.67$) or processing speed (r=–0.13, $P=0.30$). The positive association between pBGV and language processing was independent of age, sex, presence of hypertension, hyperlipidemia, diabetes mellitus, years of education, as well as pCGMV and pWMV (β=0.35; 95% CI, 0.04 to 0.66; $P=0.013$) whereas the association with verbal memory did not persist in this model (β=0.13; 95% CI, –0.23 to 0.44; $P=0.44$). There was no association between pBGV and gait velocity (r=0.02, $P=0.91$) or gait time (r=–0.13, $P=0.30$).

Discussion

Our primary finding is that CAA is associated with reduced BGV. Total BGV was reduced by 10.7% and 7.2% respectively in non-demented sporadic and hereditary CAA patients relative to age-matched HCs, with similar decreases observed in the individual volumes of putamen, caudate, and globus pallidus. BGV as a whole and the individual putamen, caudate, and globus pallidus volumes were also reduced in CAA relative to AD patients, while nucleus accumbens was smaller in AD than CAA, consistent with the high burden of AD pathology in this structure.[30] Measuring the normalized widths of caudate, putamen, and globus pallidus, we found basal ganglia atrophy in both CAA-ICH and HTN-ICH relative to HCs, but to a greater extent in CAA-ICH than HTN-ICH.

Effects of CAA on BGV are somewhat unexpected given CAA's primarily cortical and leptomeningeal localization; the current findings should therefore be considered exploratory and requiring of replication. CAA-related effects on subcortical brain regions such as the white matter, however, are well established. Amyloid positron emission tomography imaging, for example, showed a direct relationship between increasing brain amyloid burden and volume of white matter hyperintensity in non-demented CAA patients but not AD patients.[6] The mechanisms for these distant effects on subcortical brain regions remain undetermined, but could include (1) subcortical ischemia due to cortical vascular dysfunction and distal hypoperfusion and (2) subcortical neurodegeneration due to loss of cortical afferent and efferent connections. Indeed, our primary and secondary analyses together indicate that basal ganglia atrophy in CAA is to some extent in proportion to total brain volume loss, which might result either from loss of afferent and efferent connections across compartments or from correlations in the extent of injury among the brain compartments driven by overall CAA severity in each brain. An early postmortem study of eight brains with CAA noted demyelination, vacuolation, and lacunae in white matter and basal ganglia in a pattern similar to Binswanger's subcortical encephalopathy,[31] while another postmortem study of 18 brains with severe CAA found frequent microinfarcts in the white matter as well as cortical gray matter.[10] Moreover, CAA-ICH patients have previously been reported to have a similar burden of WMH as HTN-ICH[32] and in the current study demonstrate greater basal ganglia atrophy. These findings suggest that the relatively distant effects of CAA on subcortical brain structures equal or exceed those caused by arteriolosclerosis and lipohyalinosis of the more proximate deep penetrating arterioles in HTN-ICH.[33]

JoS

Fotiadis et al.   Basal Ganglia Atrophy in Cerebral Amyloid Angiopathy

We found that reduced BGV among the sporadic CAA research cohort correlated with higher basal ganglia FA. DTI-based metrics such as FA are typically studied in white matter, where higher FA is generally interpreted as indicating greater directionality of water diffusion along myelinated tracts.[34] The direction of the currently reported relationship suggests that higher FA correlates with greater basal ganglia injury, analogous to an earlier DTI study in CAA demonstrating increased FA in subthalamic gray matter relative to HCs.[8] These data raise the possibility that when measured in subcortical gray matter nuclei, increased FA may indicate greater structural injury. Indeed, this idea has also been suggested in studies of striatum and pallidum in early Huntington's disease[35] and caudate in relapsing-remitting multiple sclerosis.[36] A postulated mechanism for increased subcortical gray FA is targeted loss of dendritic connections causing restricted directional diffusion of the underlying fiber tracts.[36]

It remains to be determined whether CAA-related basal ganglia atrophy is a major contributor to the disease's clinical manifestations. Although we found relatively strong correlations between the extent of atrophy and two cognitive domains, only the association with language processing remained independent after controlling for covariates. This is noteworthy, especially considering how other types of CAA-related structural atrophy, such as white matter atrophy, affect different domains of cognitive function.[7] It could thus be speculated that basal ganglia atrophy in patients with CAA is driven by a different underlying pathological mechanism and could contribute to the disease's long-term neurocognitive dysfunction. Previous studies in neurodegenerative diseases have indeed pointed to a possible role for basal ganglia atrophy in cognitive impairment.[22,37] Given the potential for confounding by other CAA-related brain injuries,[38] however, it remains unclear whether the correlation observed among the research CAA patients indicates direct functional impact of basal ganglia atrophy.

In addition to difficulty identifying the independent contribution of basal ganglia atrophy to CAA-related clinical dysfunction, the current analysis has other limitations. Even non-demented CAA patients typically have some degree of concomitant AD pathology, raising the possibility that the identified basal ganglia atrophy is due to AD rather than CAA. We found lower caudate, putamen, globus pallidus, and total BGVs in CAA relative to AD, however, arguing against this interpretation. Similarly, basal ganglia atrophy in D-CAA should be largely unconfounded by AD pathology, as this condition has relatively few mature senile plaques and minimal neurofibrillary pathology.[39] Another limitation is the use of controls and AD scans drawn from ADNI for comparison to our CAA research and clinical cohorts, introducing the possibility of spurious differences due to variations in the MRI scans. We note that the ADNI patients were imaged using the same scanner type and magnetic field strength as the CAA group, and that the comparisons yielded basal ganglia regions that were both smaller in CAA than AD (caudate, putamen, globus pallidus) and smaller in AD than CAA (nucleus accumbens) suggesting no consistent inter-scanner bias. We also note that D-CAA patients and their matched controls were scanned on the same scanner and thus not affected by inter-scanner differences. Our analyses of HTN-ICH required a visual method for determining normalized basal ganglia width that could be applied to clinical-grade scans, potentially introducing inaccuracies in measurement relative to volumetric methods. The significant but not extremely strong correlation between the basal ganglia visual atrophy metric and the FreeSurfer-derived BGVs applied on the comparative HC cohort (r=0.22) suggests that the visual atrophy scale can be used as a basal ganglia atrophy measure when volumetric measurement is not possible, but likely introduces measurement error into the comparison of the CAA-ICH and HTN-ICH patients. The measurement error, however, would be expected to bias towards a null result rather than towards a difference between the groups. The high inter-rater reliability of the visual scale suggests that the method is reproducible and can be tested in future cohorts. Finally, all our analyses were cross-sectional using MRIs obtained at single timepoints. Longitudinal analysis of BGV will be an important future step for characterizing this process.

If confirmed in replication studies, the finding of basal ganglia atrophy would substantially extend the range of subcortical regions affected by CAA, raising challenging questions about the mechanisms for tissue injury distant from the amyloid-laden leptomeningeal and cortical vessels. Basal ganglia atrophy might also represent a novel neuroimaging marker of CAA-related brain injury. Previous studies have identified a range of candidate outcome markers for CAA, including both hemorrhagic and non-hemorrhagic brain lesions as well as alterations in vascular physiology.[40] If future studies suggest that basal ganglia injury indeed contributes to the clinical manifestations characteristic of CAA, then this marker might play an important role in interventional trials aimed at limiting CAA-related neurologic dysfunction.

Conclusions

In this case-control study, patients with sporadic or hereditary CAA displayed significant atrophy in the basal ganglia com-

pared to similar aged individuals without CAA. Moreover, CAA-related basal ganglia atrophy independently correlated with cortical gray matter atrophy, increased basal ganglia fractional anisotropy, and worse performance on language processing. Overall, the independent association of CAA with basal ganglia tissue loss could suggest a new mechanism for CAA-related brain injury and neurologic dysfunction, and a novel candidate biomarker of this currently untreatable disorder.

References

1. Wardlaw JM, Smith EE, Biessels GJ, Cordonnier C, Fazekas F, Frayne R, et al. Neuroimaging standards for research into small vessel disease and its contribution to ageing and neurodegeneration. *Lancet Neurol* 2013;12:822-838.
2. Nitkunan A, Lanfranconi S, Charlton RA, Barrick TR, Markus HS. Brain atrophy and cerebral small vessel disease: a prospective follow-up study. *Stroke* 2011;42:133-138.
3. Ikram MK, de Jong FJ, Vernooij MW, Hofman A, Niessen WJ, van der Lugt A, et al. Retinal vascular calibers associate differentially with cerebral gray matter and white matter atrophy. *Alzheimer Dis Assoc Disord* 2013;27:351-355.
4. Brundel M, van den Heuvel M, de Bresser J, Kappelle LJ, Biessels GJ; Utrecht Diabetic Encephalopathy Study Group. Cerebral cortical thickness in patients with type 2 diabetes. *J Neurol Sci* 2010;299:126-130.
5. Fotiadis P, van Rooden S, van der Grond J, Schultz A, Martinez-Ramirez S, Auriel E, et al. Cortical atrophy in patients with cerebral amyloid angiopathy: a case-control study. *Lancet Neurol* 2016;15:811-819.
6. Gurol ME, Viswanathan A, Gidicsin C, Hedden T, Martinez-Ramirez S, Dumas A, et al. Cerebral amyloid angiopathy burden associated with leukoaraiosis: a positron emission tomography/magnetic resonance imaging study. *Ann Neurol* 2013;73:529-536.
7. Fotiadis P, Reijmer YD, Van Veluw SJ, Martinez-Ramirez S, Karahanoglu FI, Gokcal E, et al. White matter atrophy in cerebral amyloid angiopathy. *Neurology* 2020;95:e554-e562.
8. Salat DH, Smith EE, Tuch DS, Benner T, Pappu V, Schwab KM, et al. White matter alterations in cerebral amyloid angiopathy measured by diffusion tensor imaging. *Stroke* 2006;37:1759-1764.
9. Reijmer YD, Fotiadis P, Martinez-Ramirez S, Salat DH, Schultz A, Shoamanesh A, et al. Structural network alterations and neurological dysfunction in cerebral amyloid angiopathy. *Brain* 2015;138(Pt 1):179-188.
10. Soontornniyomkij V, Lynch MD, Mermash S, Pomakian J, Badkoobehi H, Clare R, et al. Cerebral microinfarcts associated with severe cerebral beta-amyloid angiopathy. *Brain Pathol* 2010;20:459-467.
11. Auriel E, Edlow BL, Reijmer YD, Fotiadis P, Ramirez-Martinez S, Ni J, et al. Microinfarct disruption of white matter structure:

JoS

Fotiadis et al.   Basal Ganglia Atrophy in Cerebral Amyloid Angiopathy

a longitudinal diffusion tensor analysis. *Neurology* 2014; 83:182-188.

12. Dumas A, Dierksen GA, Gurol ME, Halpin A, Martinez-Ramirez S, Schwab K, et al. Functional magnetic resonance imaging detection of vascular reactivity in cerebral amyloid angiopathy. *Ann Neurol* 2012;72:76-81.

13. Peca S, McCreary CR, Donaldson E, Kumarpillai G, Shobha N, Sanchez K, et al. Neurovascular decoupling is associated with severity of cerebral amyloid angiopathy. *Neurology* 2013;81:1659-1665.

14. Mink JW. The basal ganglia and involuntary movements: impaired inhibition of competing motor patterns. *Arch Neurol* 2003;60:1365-1368.

15. Foerde K, Shohamy D. The role of the basal ganglia in learning and memory: insight from Parkinson's disease. *Neurobiol Learn Mem* 2011;96:624-636.

16. Booth JR, Wood L, Lu D, Houk JC, Bitan T. The role of the basal ganglia and cerebellum in language processing. *Brain Res* 2007;1133:136-144.

17. Tanaka SC, Doya K, Okada G, Ueda K, Okamoto Y, Yamawaki S. Prediction of immediate and future rewards differentially recruits cortico-basal ganglia loops. *Nat Neurosci* 2004;7:887-893.

18. Ashar YK, Andrews-Hanna JR, Dimidjian S, Wager TD. Empathic care and distress: predictive brain markers and dissociable brain systems. *Neuron* 2017;94:1263-1273.

19. Tinaz S, Courtney MG, Stern CE. Focal cortical and subcortical atrophy in early Parkinson's disease. *Mov Disord* 2011;26:436-441.

20. Cordato NJ, Halliday GM, Harding AJ, Hely MA, Morris JG. Regional brain atrophy in progressive supranuclear palsy and Lewy body disease. *Ann Neurol* 2000;47:718-728.

21. Aylward EH, Li Q, Stine OC, Ranen N, Sherr M, Barta PE, et al. Longitudinal change in basal ganglia volume in patients with Huntington's disease. *Neurology* 1997;48:394-399.

22. Hanganu A, Provost JS, Monchi O. Neuroimaging studies of striatum in cognition part II: Parkinson's disease. *Front Syst Neurosci* 2015;9:138.

23. Greenberg SM, Charidimou A. Diagnosis of cerebral amyloid angiopathy: evolution of the Boston criteria. *Stroke* 2018;49:491-497.

24. Jack CR Jr, Bernstein MA, Fox NC, Thompson P, Alexander G, Harvey D, et al. The Alzheimer's Disease Neuroimaging Initiative (ADNI): MRI methods. *J Magn Reson Imaging* 2008;27:685-691.

25. van Rooden S, van der Grond J, van den Boom R, Haan J, Linn J, Greenberg SM, et al. Descriptive analysis of the Boston criteria applied to a Dutch-type cerebral amyloid angiopathy population. *Stroke* 2009;40:3022-3027.

26. Pasi M, Boulouis G, Fotiadis P, Auriel E, Charidimou A, Haley K, et al. Distribution of lacunes in cerebral amyloid angiopathy and hypertensive small vessel disease. *Neurology* 2017;88:2162-2168.

27. Fischl B, Dale AM. Measuring the thickness of the human cerebral cortex from magnetic resonance images. *Proc Natl Acad Sci U S A* 2000;97:11050-11055.

28. Lee MJ, Kim TH, Kim SJ, Kim BK, Mun CW, Lee JH. Quantitative validation of a visual rating scale for defining high-iron putamen in patients with multiple system atrophy. *Front Neurol* 2019;10:1014.

29. Case NF, Charlton A, Zwiers A, Batool S, McCreary CR, Hogan DB, et al. Cerebral amyloid angiopathy is associated with executive dysfunction and mild cognitive impairment. *Stroke* 2016;47:2010-2016.

30. Selden N, Mesulam MM, Geula C. Human striatum: the distribution of neurofibrillary tangles in Alzheimer's disease. *Brain Res* 1994;648:327-331.

31. Gray F, Dubas F, Roullet E, Escourolle R. Leukoencephalopathy in diffuse hemorrhagic cerebral amyloid angiopathy. *Ann Neurol* 1985;18:54-59.

32. Smith EE, Nandigam KR, Chen YW, Jeng J, Salat D, Halpin A, et al. MRI markers of small vessel disease in lobar and deep hemispheric intracerebral hemorrhage. *Stroke* 2010;41:1933-1938.

33. Fisher CM. Pathological observations in hypertensive cerebral hemorrhage. *J Neuropathol Exp Neurol* 1971;30:536-550.

34. Werring DJ, Clark CA, Barker GJ, Thompson AJ, Miller DH. Diffusion tensor imaging of lesions and normal-appearing white matter in multiple sclerosis. *Neurology* 1999;52:1626-1632.

35. Douaud G, Behrens TE, Poupon C, Cointepas Y, Jbabdi S, Gaura V, et al. In vivo evidence for the selective subcortical degeneration in Huntington's disease. *Neuroimage* 2009;46:958-966.

36. Hasan KM, Halphen C, Kamali A, Nelson FM, Wolinsky JS, Narayana PA. Caudate nuclei volume, diffusion tensor metrics, and T(2) relaxation in healthy adults and relapsing-remitting multiple sclerosis patients: implications for understanding gray matter degeneration. *J Magn Reson Imaging* 2009;29:70-77.

37. Aylward EH, Harrington DL, Mills JA, Nopoulos PC, Ross CA, Long JD, et al. Regional atrophy associated with cognitive and motor function in prodromal Huntington disease. *J Huntingtons Dis* 2013;2:477-489.

38. Gurol ME, Irizarry MC, Smith EE, Raju S, Diaz-Arrastia R, Bottiglieri T, et al. Plasma beta-amyloid and white matter le-

sions in AD, MCI, and cerebral amyloid angiopathy. *Neurology* 2006;66:23-29.

39. Maat-Schieman ML, Radder CM, van Duinen SG, Haan J, Roos RA. Hereditary cerebral hemorrhage with amyloidosis (Dutch): a model for congophilic plaque formation without neurofibrillary pathology. *Acta Neuropathol* 1994;88:371-378.

40. Greenberg SM, Al-Shahi Salman R, Biessels GJ, van Buchem M, Cordonnier C, Lee JM, et al. Outcome markers for clinical trials in cerebral amyloid angiopathy. *Lancet Neurol* 2014;13: 419-428.